Partial mycoheterotrophy in the leafless orchid Eulophia zollingeri specialized on wood-decaying fungi

Suetsugu, Kenji
Ohta, Tamihisa
Tayasu, Ichiro

(Citation)
Mycorrhiza,34(1-2):33-44

(Issue Date)
2024-04

(Resource Type)
journal article

(Version)
Accepted Manuscript

Partial mycoheterotrophy in the leafless orchid *Eulophia zollingeri* specialized on wood-decaying fungi

Kenji Suetsugu[1,2*], Tamihisa Ohta[3], and Ichiro Tayasu[4]

[1]Department of Biology, Graduate School of Science, Kobe University, Kobe, Hyogo 657-8501, Japan

[2]Institute for Advanced Research, Kobe University, 1-1 Rokkodai, Nada-ku, Kobe, Hyogo 657-8501, Japan

[3]Faculty of Science, Academic Assembly, University of Toyama, Gofuku 3190, Toyama 930-8555, Japan.

[4]Research Institute for Humanity and Nature, 457-4 Motoyama, Kamigamo, Kita-ku, Kyoto, 603-8047 Japan

*corresponding author: E-mail: kenji.suetsugu@gmail.com

Abstract

Although the absence of normal leaves is often considered a sign of full heterotrophy, some plants remain at least partially autotrophic despite their leafless habit. Leafless orchids with green stems and capsules probably represent a late evolutionary stage toward full mycoheterotrophy and serve as valuable models for understanding the pathways leading to this nutritional strategy. In this study, based on molecular barcoding and isotopic analysis, we explored the physiological ecology of the leafless orchid *Eulophia zollingeri*, which displays green coloration, particularly during its fruiting phase. Although previous studies had shown that *E. zollingeri*, in its adult stage, is associated with Psathyrellaceae fungi and exhibits high ^{13}C isotope signatures similar to fully mycoheterotrophic orchids, it remained uncertain whether this symbiotic relationship is consistent throughout the orchid's entire life cycle and whether the orchid relies exclusively on mycoheterotrophy for its nutrition during the fruiting season. Our study has demonstrated that *E. zollingeri* maintains a specialized symbiotic relationship with Psathyrellaceae fungi throughout all life stages. However, isotopic analysis and chlorophyll data have shown that the orchid also engages in photosynthesis to meet its carbon needs, particularly during the fruiting stage. This research constitutes the first discovery of partial mycoheterotrophy in leafless orchids associated with saprotrophic non-rhizoctonia fungi.

Keywords autotrophy, carbon acquisition, chlorophyll, leafless orchids, mixotrophy, protocorm, saprotrophic fungi, stable isotopes

Introduction

41 Orchidaceae, the most species-rich family in angiosperms, is renowned for its tiny seeds
42 with minimal nutrients (Arditti and Ghani 2000). These plants rely entirely on
43 mycorrhizal fungi for their carbon needs during their early underground growth, a
44 phenomenon known as mycoheterotrophy (Leake 1994). Phylogenetic studies have
45 revealed that the loss of photosynthesis in adulthood, coupled with full
46 mycoheterotrophy, has independently occurred at least 40 times within Orchidaceae
47 (Merckx and Freudenstein 2010; Jacquemyn and Merckx 2019). Recent advancements
48 in our understanding of these intriguing plants have been facilitated by the application
49 of molecular and isotopic approaches.

50 Stable isotope analysis is a crucial method for assessing orchid nutrition, relying
51 on two key observations: (i) Fungal tissues are enriched in heavy carbon and nitrogen
52 isotopes compared to autotrophic plants (Gebauer and Dietrich 1993; Gleixner et al.
53 1993). (ii) Fully mycoheterotrophic orchids have isotopic signatures similar to or
54 slightly higher than their fungal partners (Gebauer and Meyer 2003; Trudell et al. 2003).
55 Gebauer & Meyer (2003) discovered that some green species of *Cephalanthera* and
56 *Epipactis* exhibit higher ^{13}C and ^{15}N levels compared to nearby autotrophic plants, yet
57 these levels are lower than those in fully mycoheterotrophic plants. This indicates
58 partial mycoheterotrophy, a mixotrophic nutritional mode that combines autotrophy and
59 mycoheterotrophy in the adult stage (Gebauer and Meyer 2003). Partial
60 mycoheterotrophy has later been recognized in a wide array of orchids in most orchid
61 subfamilies, including the basal clade (Bidartondo et al. 2004; Julou et al. 2005;
62 Motomura et al. 2010; Gebauer et al. 2016; Suetsugu and Matsubayashi 2021a;
63 Suetsugu et al. 2021b, c).

64 Furthermore, molecular identifications of mycobionts have established a clear

link between the nutritional modes of orchids and their fungal associations. Most green orchids associate with 'rhizoctonias' basidiomycetes, including Ceratobasidiaceae, Tulasnellaceae, and Serendipitaceae (Dearnaley et al. 2013; Rasmussen and Rasmussen 2014). However, fully mycoheterotrophic orchids, except for albino variants, specialize in associations with ectomycorrhizal or saprotrophic non-rhizoctonia fungi (Jacquemyn and Merckx 2019; Ogura-Tsujita et al. 2021). Additionally, in line with their intermediate isotopic signatures, partially mycoheterotrophic orchids with a relatively high degree of mycoheterotrophy also tend to affiliate with these fungi (Bidartondo et al. 2004; Selosse and Roy 2009; Hynson et al. 2013; Suetsugu et al. 2022). This suggests that the transition to exploiting ectomycorrhizal fungi or saprotrophic non-rhizoctonia fungi likely occurred before the loss of photosynthesis (Selosse and Roy 2009; Motomura et al. 2010; Jacquemyn and Merckx 2019; Suetsugu et al. 2022).

During the evolution of full mycoheterotrophy, another prominent trend has been the substantial reduction of leaves (Merckx et al. 2013; Tsukaya 2018). Notably, lineages of partial mycoheterotrophs exhibit a range of leaf development. Some species, such as *Cephalanthera damasonium* and *Epipactis helleborine*, retain well-developed foliage leaves (Julou et al. 2005; Stöckel et al. 2011; Suetsugu et al. 2017). In contrast, others, such as *Cephalanthera subaphylla*, *Epipactis microphylla*, and *Stigmatodactylus sikokianus*, produce highly reduced ones (Selosse et al. 2004; Sakamoto et al. 2016; Suetsugu et al. 2021a). The presence of these diverse phenotypes suggests that the process of leaf reduction during evolution was gradual rather than the result of a single-step mutation (Roy et al. 2013).

Moreover, some orchids, such as *Limodorum abortivum*, *Cymbidium macrorhizon*, and *Corallorhiza trifida*, lack foliage leaves but maintain green stems and capsules.

While these leafless orchids have often been presumed to be fully mycoheterotrophic, several studies have indicated that they retain some degree of autotrophic capacity (Girlanda et al. 2005; Zimmer et al. 2008; Cameron et al. 2009). For instance, chlorophyll accumulation has been found in shoots and capsules of *C. macrorhizon*, especially during fruiting (Suetsugu et al. 2018; Kobayashi et al. 2021). Using a linear two-source mixing model with sprouting plants as 100% carbon gain from fungi and autotrophic plants as the 0% baseline, Suetsugu et al. (2018) estimated that fruiting *C. macrorhizon* plants obtain about 25% of their total carbon from autotrophy.

While their contribution to net carbon acquisition may be limited, leafless orchids with green stems and capsules likely represent a late stage in the evolution of full mycoheterotrophy, offering valuable models for understanding the pathways leading to complete heterotrophy (Cameron et al. 2009; Suetsugu et al. 2018; Kobayashi et al. 2021). For instance, although fully mycoheterotrophic plants often exhibit higher mycorrhizal specificity than partially mycoheterotrophic ones (Hynson et al. 2013; Jacquemyn and Merckx 2019), these leafless species with reduced photosynthetic ability also tend to associate predominantly with narrow clades of ectomycorrhizal fungi (Girlanda et al. 2005; Zimmer et al. 2008; Ogura-Tsujita et al. 2012). This specialization mirrors that in fully mycoheterotrophic plants, indicating a closer physiological state to full mycoheterotrophy. However, the evolution of mycoheterotrophy involving saprotrophic non-rhizoctonia fungi is less understood. Although some orchids with developed foliage leaves are shown to exhibit partial mycoheterotrophy with saprotrophic non-rhizoctonia fungi (Suetsugu and Matsubayashi 2021b; Yagame et al. 2021; Zahn et al. 2022; Suetsugu et al. 2022), leafless orchids with green stems and capsules associated with these fungi, potentially representing further intermediate stages,

113 are yet to be discovered.

114 To gain deeper insights into the diverse nutritional strategies employed by orchids,
115 our study focused on *E. zollingeri*, a leafless orchid species characterized by faintly
116 green stems. This species is part of the pantropical genus *Eulophia*, which includes
117 approximately 230 species (Merckx et al. 2013). While most *Eulophia* species are
118 terrestrial, a few can be found as epiphytes or lithophytes. Notably, at least 17 species
119 within this genus lack leaves and are considered fully mycoheterotrophic (Merckx et al.
120 2013). Examples of these leafless species include *E. epiphanoides* in southwest
121 Tanzania, *E. galeoloides* in tropical Africa, *E. gastrodioides* in Mozambique and
122 Zambia, *E. macrantha* in Malawi and Zimbabwe, *E. richardsiae* in northern Zambia,
123 and *E. zollingeri*, which is widespread across tropical and subtropical regions in Asia
124 and Australia (Merckx et al. 2013).

125 Despite its wide distribution, *E. zollingeri* establishes a specialized association
126 with a specific lineage of wood-decaying Psathyrellaceae fungi at least at the adult stage
127 (Ogura-Tsujita and Yukawa 2008). This species is often considered to be fully
128 mycoheterotrophic due to its lack of foliage leaves and violet stem coloration during the
129 flowering stage (Ogura-Tsujita and Yukawa 2008; Ogura-Tsujita et al. 2021). This
130 classification is further supported by its high $\delta^{13}C$ values (Suetsugu et al. 2020). Yet, its
131 deeper green hue in the fruiting stage suggests chlorophyll accumulation, indicating
132 possible partial autotrophy. Our study aimed to clarify the trophic status of *E. zollingeri*
133 at different developmental stages, including protocorm, flowering, and fruiting stages,
134 by analyzing $\delta^{13}C$ and $\delta^{15}N$ isotopic signatures. Additionally, we measured chlorophyll
135 content and chlorophyll fluorescence to accurately assess the nutritional mode of this
136 species. Finally, we investigated the fungal partners of *E. zollingeri* during these stages

using high-throughput DNA sequencing.

Materials and Methods

Study site and sampling procedures

Fieldwork was conducted in an evergreen broad-leaved forest located in Miyazaki City, Miyazaki Prefecture, Japan. Two visits were made to the site: the first on July 9, 2017, during the flowering season, and the second on September 16, 2017, during the fruiting season. The forest was predominantly composed of *Castanopsis sieboldii* trees, and the study population included approximately 30 individuals of *E. zollingeri* (Fig. 1).

At the study site, we collected stem tips, each approximately 3 centimeters long, from both flowering (n = 8) and fruiting (n = 8) individuals of *E. zollingeri.* These samples were then analyzed for chlorophyll content and isotopic composition. In addition, we gathered leaves from co-occurring autotrophic reference species for isotopic analysis. To minimize the influence of environmental variables, such as atmospheric CO_2 isotope composition, microscale light conditions, and soil type (Gebauer and Schulze 1991), we collected leaves from reference plants growing in close spatial proximity (< 1 m) at the same height as the focal *E. zollingeri* individuals. This criterion led us to select *C. sieboldii* and *Neolitsea sericea*, as they were the only plants growing in close spatial proximity with the same distance from the ground.

Additionally, we collected mycorrhizal samples from flowering individuals (n = 5) and fruiting individuals (n = 5) for molecular identification of mycorrhizal fungi. To minimize the sampling impact, we extracted the minimum required root samples, harvesting 2−4 root fragments by excavating soil about 10 cm away from the shoots and

161 approaching the plant underground from one side. After sampling, the excavated holes
162 were refilled with the same soil composition. During the process, we fortuitously
163 collected *E. zollingeri* protocorms near four individual *E. zollingeri* individuals at the
164 fruiting season. These protocorms, originating around the same *E. zollingeri* individuals,
165 were then combined and used for both mycobiont molecular identification and isotopic
166 analysis.
167
168 **Chlorophyll measurement**
169 To measure chlorophyll fluorescence, both flowering (n = 8) and fruiting (n = 8)
170 individuals of *E. zollingeri* were dark-adapted for 15 minutes. Following this, the
171 steady-state quantum yield of photosystem II was assessed using a FluorPen FP100
172 (Photon Systems Instruments, Brno, Czech Republic). This value was defined as the
173 ratio of the actual fluorescence yield (Fv) to the maximum fluorescence (Fm).
174 Chlorophyll concentrations were measured following the methodology of Zimmer
175 et al. (2008). Briefly, we collected the tips of stems from flowering or fruiting *E.*
176 *zollingeri* specimens and finely cut them using small scissors and a surgical knife.
177 Approximately half of each sample was allocated for chlorophyll measurement, while
178 the remaining portion was used for stable isotope analysis. The finely chopped samples
179 designated for chlorophyll measurement were mixed with N, N'-dimethylformamide
180 and stored in the dark at –23°C for 8 days after recording their fresh weight. After
181 centrifugation, the absorbance levels of the supernatants at 646.8, 663.8, and 750 nm
182 were measured using a spectrophotometer (U-2010; Hitachi High Technologies, Tokyo,
183 Japan). Chlorophyll concentrations were calculated according to the equation outlined
184 by Porra *et al.* (1989):

185

186 Chl*a* (μg/mg FW) = $12.00(A_{663.8} - A_{750}) - 3.11(A_{646.8} - A_{750})$

187 Chl*b* (μg/mg FW) = $20.78(A_{646.8} - A_{750}) - 4.88(A_{663.8} - A_{750})$

188

189 where *A* represents absorbance at the specified wavelengths. Total chlorophyll
190 concentration (Chl*a* + *b*) is expressed on a fresh mass basis (μg/mg FW). Differences in
191 chlorophyll fluorescence and chlorophyll concentration between the flowering and
192 fruiting stages of *E. zollingeri* were analyzed using Student's t-test.

193

194 **Molecular identification of mycobionts**

195 Excised roots or protocorms were examined under a light microscope to confirm
196 mycorrhizal colonization. For molecular analysis, mycorrhizal fragments filled with
197 fungal pelotons (measuring 3–5 mm in length) were collected from each *E. zollingeri*
198 sample. Following surface sterilization, DNA was extracted from these mycorrhizal
199 samples using the cetyltrimethylammonium bromide method (Doyle and Doyle 1990).

200 The nuclear ribosomal internal transcribed spacer 2 (ITS2) region was amplified
201 using a basidiomycetes-specific primer set, following the methodology outlined by
202 Suetsugu and Matsubayashi (2021b). The first round of polymerase chain reaction
203 (PCR) utilized the primer set ITS1OF/ITS4OF (Taylor and McCormick 2008) and was
204 conducted under the following cycle conditions: an initial denaturation at 98°C for 3
205 minutes, followed by 35 cycles of 98°C for 10 seconds, 58°C for 20 seconds, and 72°C
206 for 20 seconds, with a final extension at 72°C for 10 minutes. The Q5 High-Fidelity
207 DNA Polymerase Kit (NEB, Ipswich, USA) was used for this process. Nested PCR was
208 also performed using the primer set ITS86F/ITS4 (Waud et al. 2014), which was fused

209 with 3–6-mer Ns and with Illumina forward/reverse sequencing primers. DNA
210 metabarcoding with the selected primer pair (ITS86F/ITS4) is known to be highly
211 suitable for studying mycorrhizal communities of orchids (e.g., Op De Beeck et al.
212 2014; Waud et al. 2014). The same polymerase kit was used under the following cycle
213 conditions: an initial denaturation at 98°C for 3 minutes, followed by 10 cycles of 98°C
214 for 10 seconds, 65°C for 20 seconds, and 72°C for 20 seconds, with a final extension at
215 72°C for 10 minutes.
216 Supplemental PCR was additionally performed to incorporate Illumina P5/P7
217 adapter sequences and sample-specific indices (Syed et al. 2009; Suetsugu and
218 Matsubayashi 2021a). The resulting ITS sequencing libraries were processed using an
219 Illumina MiSeq sequencer, equipped with a 2 × 150 cycle sequencing kit (10% PhiX
220 spike-in; Illumina, San Diego, CA, USA). The raw sequence data were deposited in the
221 DRA (accession number DRA017590).
222 Bioinformatic analysis was carried out using Claident v.0.2.2019.05.10 (Tanabe
223 and Toju 2013), as described by Suetsugu *et al.* (2021b) and Suetsugu and
224 Matsubayashi (2021b). Briefly, operational taxonomic units (OTUs) were defined based
225 on a sequence similarity cutoff of 97%, and potentially chimeric OTUs were eliminated
226 using UCHIME version 7.2 (Nilsson et al. 2019). Taxonomic assignments of the OTUs
227 were conducted using the query-centric auto-*k*-nearest-neighbor (QCauto) and lowest
228 common ancestor algorithms (Tanabe and Toju 2013). The most abundant sequence
229 within each OTU cluster was designated as the representative sequence for that OTU.
230 Because all *E. zollingeri* specimens were predominantly colonized by OTUs
231 classified within the family Psathyrellaceae, a phylogenetic tree comprising the detected
232 Psathyrellaceae OTUs and closely related fungi was constructed. Specifically, the OTUs

identified as *E. zollingeri* mycobionts were queried against the International Nucleotide Sequence Database Collaboration (INSDC) using BLAST (Altschul et al. 1997). Several phylogenetically close sequences, along with other representative sequences from the family Psathyrellaceae, were downloaded. Finally, these sequences were aligned using ClustalW, and a maximum-likelihood tree was constructed using MEGA X (Kumar et al. 2018) using the maximum likelihood (ML) method with a GTR + I + G model and 1,000 bootstrap replicates.

$\delta^{13}C$ and $\delta^{15}N$ analysis

The natural abundance of ^{13}C and ^{15}N isotopes in the *E. zollingeri* and co-occurring autotrophic reference plants was measured using a continuous-flow isotope-ratio mass spectrometer connected to an elemental analyzer (Thermo Fisher Scientific, Waltham, Massachusetts, USA), as described by Suetsugu and Matsubayashi (2021b). Relative isotope abundances were calculated and denoted as:

$$\delta^{13}C \text{ or } \delta^{15}N = (R_{sample}/R_{standard} - 1) \times 1{,}000\ [‰],$$

where R_{sample} represents the $^{13}C/^{12}C$ or $^{15}N/^{14}N$ ratio of each sample, and $R_{standard}$ represents the $^{13}C/^{12}C$ or $^{15}N/^{14}N$ ratios of Vienna PeeDee belemnite or atmospheric N_2, respectively. The C and N isotope ratios were calibrated using the following laboratory standards: CERKU-01 (DL-alanine, $\delta^{13}C = -25.36‰$, $\delta^{15}N = -2.89‰$), CERKU-02 (L-alanine, $\delta^{13}C = -19.04‰$, $\delta^{15}N = 22.71‰$) and CERKU-05 (L-threonine, $\delta^{13}C = -9.45‰$, $\delta^{15}N = -2.88‰$) for C, and CERKU-01 and CERKU-02 for N (Tayasu et al. 2011). The analytical standard deviations (SD) of these standards were 0.03‰ ($\delta^{13}C$, n

= 5) and 0.06‰ ($\delta^{15}N$, n = 5) for DL-alanine, 0.04‰ ($\delta^{13}C$, n = 5) and 0.07‰ ($\delta^{15}N$, n = 5) for L-alanine, and 0.03‰ ($\delta^{13}C$, n = 5) for L-threonine.

To facilitate seasonal comparisons, we employed a conversion of δ values into site-independent enrichment factors (ε) for both seasons. Initially, we computed the average $\delta^{13}C$ and $\delta^{15}N$ values for reference plants within each season. Subsequently, we subtracted these average values from the respective $\delta^{13}C$ and $\delta^{15}N$ values of the *E. zollingeri* samples and reference plants, resulting in site-independent enrichment factors ($\varepsilon = \delta^{x}S - \delta^{x}R$) for each sample. Here, $\delta^{x}S$ represents the $\delta^{13}C$ or $\delta^{15}N$ value of a specific *E. zollingeri* specimen, and $\delta^{x}R$ signifies the mean $\delta^{13}C$ or $\delta^{15}N$ of all reference plants within the same season.

To determine the proportion of carbon derived from fungi (% Cdf) in fruiting *E. zollingeri* specimens, we applied a linear two-source mixing model: % Cdf = ($\varepsilon^{13}C_{fruit}/\varepsilon^{13}C_{FMH}$) × 100. In this equation, $\varepsilon^{13}C_{fruit}$ corresponds to the ^{13}C enrichment factor of a fruiting *E. zollingeri* plant, while $\varepsilon^{13}C_{FMH}$ represents the mean ^{13}C enrichment factor of *E. zollingeri* at the protocorm stage or the flowering stage.

After verifying the normal distribution of the $\delta^{13}C$, $\delta^{15}N$, $\varepsilon^{13}C$, and $\varepsilon^{15}N$ datasets with Bartlett's test, the variations in their values among protocorms, flowering, and fruiting individuals were assessed through a one-way ANOVA. Subsequently, post-hoc multiple comparisons were conducted among them using the Tukey-Kramer test.

Results

Chlorophyll fluorescence and concentration

The total chlorophyll concentrations (Chl*a* + *b*) of fruiting *E. zollingeri* individuals were

quantified at 80.3 ± 10.0 μg gFW−1 (mean ± SD), while their flowering counterparts exhibited a concentration of 29.1 ± 5.2 μg gFW−1. Statistical analysis revealed a significant difference, with the chlorophyll concentration of fruiting *E. zollingeri* individuals significantly higher than that of the flowering *E. zollingeri* individuals ($P < 0.001$). However, there was no significant difference in the Chl*a*: Chl*b* ratios between the flowering (2.0 ± 0.1) and fruiting (2.1 ± 0.1) specimens ($P = 0.21$).

Simultaneously, the evaluation of the maximum quantum yield of photosystem II (Fv/Fm) revealed that the flowering *E. zollingeri* specimens exhibited a value of 0.65 ± 0.04, similar to the value recorded for the fruiting *E. zollingeri* specimens at 0.67 ± 0.04 ($P = 0.37$). However, the mean Fv/Fm values recorded in *E. zollingeri* during both the flowering and fruiting stages were lower than the typical range of 0.7−0.83 observed in normal autotrophic plants (Maxwell and Johnson 2000; Ritchie 2006). Despite this, as Ritchie (2006) suggests, these Fv/Fm values are not so depressed as to imply the complete absence of photosynthesis. This finding confirms that *E. zollingeri* maintains a PSII apparatus that, while somewhat degenerated, remains functional.

Molecular identification of mycobionts

Fungal ITS sequences were successfully obtained from a total of 22 mycorrhizal samples collected from 14 *E. zollingeri* specimens. As expected, *E. zollingeri* was predominantly associated with wood-decaying fungi from the Psathyrellaceae family throughout the entire life cycle (Fig. 2; Table S1).

Following quality-filtering, our analysis revealed the presence of five OTUs, accounting for a total of 22,629 sequencing reads in mycorrhizal tissues of *E. zollingeri* during the protocorm stage. Two of these OTUs, encompassing 17,454 reads

305 (constituting 77.1% of all reads), were assigned to the family Psathyrellaceae. A similar
306 pattern emerged in mycorrhizal tissues of *E. zollingeri* during the flowering stage,
307 where 15 OTUs (64,390 sequencing reads) were identified, with seven OTUs
308 (comprising 61,346 reads, 95.3% of all reads) attributed to Psathyrellaceae. Similarly,
309 22 OTUs (68,970 sequencing reads) were detected in mycorrhizal tissues of *E.*
310 *zollingeri* during the fruiting stage, with eight OTUs (accounting for 54,229 reads,
311 78.6% of all reads) belonging to Psathyrellaceae.

312 Given the predominance of Psathyrellaceae in the mycobionts of *E. zollingeri*, we
313 conducted a phylogenetic analysis using representative sequences of the OTUs obtained
314 from our study and closely related Psathyrellaceae species. The ML phylogenetic
315 analysis demonstrated that the dominant OTUs in *E. zollingeri* formed a clade with the
316 mycobionts previously identified in *E. zollingeri*, specifically within the
317 *Candolleomyces candolleanus* (= *Psathyrella candolleana*) species complex (Fig. 3).
318 This clade also included the mycobionts of an unrelated fully mycoheterotrophic orchid
319 *Epipogium roseum.*

320

321 **Stable isotope analysis**

322 The $\delta^{13}C$ values of *E. zollingeri* specimens during the fruiting stage (−25.8 ± 0.4‰)
323 were significantly lower than those of *E. zollingeri* specimens during both the
324 protocorm stage (−25.2 ± 0.4‰; $P < 0.05$; Fig. 4) and during the flowering stage (−25.0
325 ± 0.3‰; $P < 0.01$). On the other hand, there were no significant differences in the $\delta^{13}C$
326 values of neighboring autotrophic reference plants sampled during the flowering stage
327 (−32.6 ± 1.0‰) and the fruiting stage (−32.1 ± 1.2‰; $P = 0.37$). Consequently, the $\varepsilon^{13}C$
328 values of *E. zollingeri* specimens during the fruiting stage (6.4 ± 0.4‰) were

329 significantly lower than those observed in *E. zollingeri* specimens during the protocorm
330 stage (6.9 ± 0.4‰; $P < 0.05$) or the flowering stage (7.6 ± 0.3‰; $P < 0.001$; Table S2).
331 Using the mean $\varepsilon^{13}C$ values of *E. zollingeri* specimens during the protocorm stage
332 as a reference point for fully mycoheterotrophic conditions, we estimated that *E.*
333 *zollingeri* specimens at the fruiting stage derived approximately 92.0 ± 5.2% of their
334 organic matter from mycorrhizal fungi. Meanwhile, when employing the mean $\varepsilon^{13}C$
335 values of *E. zollingeri* specimens during the flowering stage as a reference for fully
336 mycoheterotrophic conditions, it was calculated that E. zollingeri obtains approximately
337 83.9 ± 4.8% of its carbon from the fungal association during the fruiting stage.
338 In contrast, there were no statistically significant disparities observed in the $\delta^{15}N$
339 values between the flowering (2.5 ± 1.3‰) and fruiting stages of *E. zollingeri* (2.2 ±
340 1.5‰; $P = 0.75$; Fig. 4). Additionally, both stages exhibited significantly elevated $\delta^{15}N$
341 values in comparison to the protocorms (0.1 ± 0.3‰; $P < 0.05$). Similarly, the $\varepsilon^{15}N$
342 values of *E. zollingeri* specimens during the flowering (5.4 ± 1.3‰) or fruiting stage
343 (6.3 ± 1.5‰) were significantly higher than those observed in *E. zollingeri* specimens
344 during the protocorm stage (4.2 ± 0.3‰; $P < 0.05$).
345
346 **Discussion**
347 The evolutionary process of full mycoheterotrophy involving saprotrophic
348 non-rhizoctonia fungi has been poorly understood, and it was only recently revealed that
349 certain orchids with well-developed foliage leaves exhibit partial mycoheterotrophy
350 with these fungi. This study marks the first discovery of partial mycoheterotrophy
351 among leafless orchids associated with saprotrophic non-rhizoctonia fungi, potentially
352 representing further stages toward full mycoheterotrophy.

353 Molecular identification in our study revealed that *E. zollingeri* is predominantly
354 colonized by Psathyrellaceae fungi throughout its entire life cycle. These findings align
355 with previous research indicating that *E. zollingeri* adult plants are exclusively
356 associated with the *C. candolleanus* species complex across regions spanning Japan,
357 Myanmar, and Taiwan (Ogura-Tsujita and Yukawa 2008). Our findings expand the
358 understanding of the partnership across different life stages, going beyond previous
359 studies targeting mycorrhizal communities during the adult stage (Ogura-Tsujita and
360 Yukawa 2008; Suetsugu et al. 2020).

361 In addition, our molecular analysis suggests that *E. zollingeri* may form
362 simultaneous associations with ectomycorrhizal families such as Sebacinaceae,
363 Thelephoraceae, and Russulaceae during certain stages of its life cycle. Interestingly,
364 ectomycorrhizal Sebacinaceae and Russulaceae are predominantly associated with
365 leafless orchids closely related to *E. zollingeri*, such as *Cymbidium macrorhizon* and
366 *Cymbidium aberrans*, which are also members of the tribe Cymbidieae (Ogura-Tsujita
367 et al. 2012). However, due to the limited sequence reads in our study and the lack of
368 information on peloton formation by these fungi, it remains unknown whether ECM
369 associations contribute to the carbon budget of *E. zollingeri.* Overall, we consider that
370 the wood-decaying *Candolleomyces* likely plays a significant role in the carbon supply
371 of *E. zollingeri*, given its dominant association. This is supported by previous studies
372 showing the predominant association of the *C. candolleanus* species complex with adult
373 plants of *E. zollingeri* (Ogura-Tsujita and Yukawa 2008) and the high ^{14}C enrichment
374 pattern in *E. zollingeri*, which reflects ^{14}C-enriched bomb carbon from deadwood
375 (Suetsugu et al. 2020).

376 The comparison of ^{13}C isotopic data showed that fruiting *E. zollingeri* individuals

377 are characterized by a lower enrichment in ^{13}C, suggesting the contribution of
378 photosynthesis to its C nutrition. Recent studies involving stable isotope analysis have
379 also suggested the capacity for photosynthesis in leafless orchids with
380 chlorophyll-containing stems (Zimmer et al. 2008; Suetsugu et al. 2018). On the other
381 hand, we note that mycoheterotrophic plants and their fungal partners exhibit
382 tremendous variations in their C and N isotope profiles, influenced by their distinct
383 physiological characteristics, such as soil nutrient acquisition strategies (Mayor et al.
384 2009; Hynson et al. 2016; Schiebold et al. 2017; Zahn et al. 2023). These variations can
385 mask the actual contributions of photosynthesis and mycoheterotrophy, potentially
386 leading to inaccuracies in determining the nutritional mode of some leafless orchids.
387 Therefore, to accurately assess the ecophysiology of such orchids, it is crucial to
388 measure stable isotope abundance throughout their entire life cycle, ideally including
389 analysis at the fully mycoheterotrophic stage (Schweiger et al. 2018; Suetsugu et al.
390 2018). In this context, our study, which distinctly focuses on both flowering plants with
391 low chlorophyll expression and the protocorm stage of the same species collected from
392 the same site, presents several advantages over previous research in this field.

393 In our assessment, which utilizes flowering *E. zollingeri* plants with minimal
394 chlorophyll accumulation as a reference for fully mycoheterotrophic status, we estimate
395 that *E. zollingeri* obtains approximately 16% of its carbon through autotrophy during
396 the fruiting stage. However, this method might underestimate the contribution of fungal
397 associations to the carbon gain in fruiting *E. zollingeri.* This potential underestimation
398 arises because (1) photosynthates acquired during previous years can be stored in the
399 underground structures of flowering *E. zollingeri* plants, and (2) these plants may
400 already perform low levels of photosynthesis (Suetsugu et al. 2018).

401 Therefore, it might be more appropriate to use the non-photosynthetic
402 underground protocorm stage as the fully mycoheterotrophic endpoint. However,
403 protocorms consist of both plant and mycorrhizal fungi, leading to intermediary isotope
404 ratios between mycoheterotrophic plants and fungi. Given the systematic increase in ^{13}C
405 and ^{15}N abundance at each trophic level within a food chain (DeNiro and Epstein 1976),
406 the isotopic composition of mycoheterotrophic plants often exceeds the $\delta^{13}C$ and $\delta^{15}N$
407 values found in their associated fungi (Schiebold et al. 2017). Therefore, using
408 protocorms as a fully mycoheterotrophic reference may also result in underestimation
409 (Johansson et al. 2015). In fact, when using the $\varepsilon^{13}C$ values of *E. zollingeri* protocorms
410 as a fully mycoheterotrophic endpoint, it was estimated that fruiting stage specimens
411 derived only 8% of their carbon via photosynthesis. Yet, all eight fruiting individuals of
412 *E. zollingeri* exhibited slightly lower $\varepsilon^{13}C$ values, indicating some degree of autotrophic
413 contribution. Thus, despite challenges in precisely estimating the level of
414 mycoheterotrophy, our study provides evidence for partial autotrophy in *E. zollingeri.*
415 It is also noteworthy that the $\varepsilon^{15}N$ values of flowering or fruiting *E. zollingeri*
416 specimens were significantly higher than those observed in *E. zollingeri* protocorms.
417 This difference is likely influenced by the presence of fungal tissue within the
418 protocorm. Notably, the average ^{15}N enrichment from mycobionts to fully
419 mycoheterotrophic orchids (Zahn et al. 2023) often surpasses the typical increase of
420 2.2–3.4‰ in $\delta^{15}N$ values observed in consumers relative to their diet (Minagawa and
421 Wada 1984; Zanden and Rasmussen 2001; McCutchan Jr et al. 2003). This notable
422 enrichment pattern could be attributed to the selective incorporation of ^{15}N-enriched
423 nitrogen by orchids (Gomes et al. 2023; Zahn et al. 2023). Our observations of *E.*
424 *zollingeri* further corroborate this, providing indirect evidence for the selective transport

425 of ^{15}N-enriched nitrogen from mycobionts to the orchid.

426 Chlorophyll analysis has shown that *E. zollingeri* does produce chlorophyll, but
427 the amount is relatively low, constituting approximately 1–3% of the levels typically
428 found in the leaves of green understory orchids (Julou et al. 2005; Suetsugu and
429 Matsubayashi 2022). Nonetheless, there is an accumulation of chlorophyll in *E.*
430 *zollingeri* during its fruiting stage, possibly indicating a shift towards partial autotrophy,
431 a notion supported by the observed ^{13}C enrichment pattern. We also detected
432 chlorophyll-dependent photochemical activity, specifically in photosystem II. Although
433 low Fv/Fm values indicate suboptimal light utilization and reduced efficiency of
434 photosystem II, these values do not suggest a complete absence of photosynthesis
435 (Ritchie 2006). The similarity between the plastome of *E. zollingeri* and other
436 photosynthetic orchids with well-developed leaves further supports the hypothesis that
437 this species retains some photosynthetic capabilities (Kim et al. 2020). Given the strong
438 induction of chlorophyll accumulation and the δ^{13}C values observed during the fruiting
439 stage, *E. zollingeri* arguably engages in partial autotrophy at this stage, with
440 photosynthesis likely contributing to seed production.

441 Interestingly, some leafless orchids such as *Limodorum abortivum* (Neottieae) and
442 *C. macrorhizon* (Cymbidieae) also accumulate chlorophyll during the fruiting season
443 (Bellino et al. 2014; Suetsugu et al. 2018). These trends suggest that the use of
444 photosynthesis for reproductive purposes is a recurring strategy across different
445 phylogenetic lineages of orchids. Such reliance on photosynthates could even act as a
446 constraint potentially hindering the transition from partial to full mycoheterotrophy.

447 In summary, our study demonstrates that the leafless orchid *E. zollingeri*
448 maintains a specialized relationship with Psathyrellaceae fungi, which probably plays a

critical role in providing it with a carbon supply throughout its entire life cycle. However, our investigation, using isotopic and chlorophyll fluorescence data, revealed that this orchid still performs photosynthesis during its fruiting stage. These findings support the hypothesis that transitions to mycoheterotrophy are achieved through a gradual increase in the level of mycoheterotrophy, rather than by abrupt shifts of trophic mode (Selosse and Roy 2009; Motomura et al. 2010; Jacquemyn and Merckx 2019; Suetsugu et al. 2022). Our research has added another piece to the understanding of the spectrum of nutritional strategies among partially mycoheterotrophic plants, ranging from almost complete autotrophy to nearly complete mycoheterotrophy.

Data availability

The sequence data have been deposited in the Sequence Read Archive of the DNA Data Bank of Japan (accession no. DRA017590). Additional supporting information is available online in the Supporting Information section at the end of the article.

Acknowledgements

The authors thank Nobuyuki Inoue and Tadashi Minamitani for their invaluable support during the field studies. We also thank Hidehito Okada, Kazuma Takizawa, and Takako Shizuka for their technical assistance.

Funding information

This study was financially supported by PRESTO (JPMJPR21D6, KS) from the Japan Science and Technology Agency and the JSPS KAKENHI (16H02524, IT and 17H05016, KS), and a Joint Research Grant for the Environmental Isotope Study of

Research Institute for Humanity and Nature.

Author contributions

KS planned and designed the research, conducted field and laboratory experiments, carried out analyses, and wrote the initial draft. TO conducted isotopic experiments, performed analyses, and contributed to manuscript revisions. IT supervised the isotopic experiments conducted by TO and revised the manuscript. All authors have approved the final version.

References

Altschul SF, Madden TL, Schäffer AA, et al (1997) Gapped BLAST and PSI-BLAST: a new generation of protein database search programs. Nucleic Acids Research 25:3389–3402. https://doi.org/10.1093/nar/25.17.3389

Arditti J, Ghani AKA (2000) Numerical and physical properties of orchid seeds and their biological implications. New Phytol 145:367–421

Bellino A, Alfani A, Selosse MA, et al (2014) Nutritional regulation in mixotrophic plants: new insights from *Limodorum abortivum*. Oecologia 175:875–885. https://doi.org/10.1007/s00442-014-2940-8

Bidartondo MI, Burghardt B, Gebauer G, et al (2004) Changing partners in the dark: isotopic and molecular evidence of ectomycorrhizal liaisons between forest orchids and trees. Proc R Soc Lond B 271:1799–1806. https://doi.org/10.1098/rspb.2004.2807

Cameron DD, Preiss K, Gebauer G, Read DJ (2009) The chlorophyll-containing orchid *Corallorhiza trifida* derives little carbon through photosynthesis. New Phytologist 183:358–364. https://doi.org/10.1111/j.1469-8137.2009.02853.x

Dearnaley JDW, Martos F, Selosse MA (2013) Orchid mycorrhizas: Molecular ecology, physiology, evolution and conservation aspects. In: Hock B (ed) Fungal associations. Springer, Berlin, Germany, pp 207–230

501 DeNiro MJ, Epstein S (1976) You are what you eat (plus a few ‰): The carbon isotope
502 cycle in food chains. Geological Society of America Abstracts with Programs
503 8:834–835

504 Doyle JJ, Doyle JL (1990) Isolation of plant DNA from fresh tissue. Focus 12:13–15

505 Gebauer G, Dietrich P (1993) Nitrogen isotope ratios in different compartments of a
506 mixed stand of spruce, larch and beech trees and of understorey vegetation
507 including fungi. Isotopes in Environmental and Health Studies 29:35–44

508 Gebauer G, Meyer M (2003) ^{15}N and ^{13}C natural abundance of autotrophic and
509 myco-heterotrophic orchids provides insight into nitrogen and carbon gain from
510 fungal association. New Phytologist 160:209–223.
511 https://doi.org/10.1046/j.1469-8137.2003.00872.x

512 Gebauer G, Preiss K, Gebauer AC (2016) Partial mycoheterotrophy is more widespread
513 among orchids than previously assumed. New Phytol 211:11–15.
514 https://doi.org/10.1111/nph.13865

515 Girlanda M, Selosse MA, Cafasso D, et al (2005) Inefficient photosynthesis in the
516 Mediterranean orchid *Limodorum abortivum* is mirrored by specific association
517 to ectomycorrhizal Russulaceae. Molecular Ecology 15:491–504.
518 https://doi.org/10.1111/j.1365-294X.2005.02770.x

519 Gleixner G, Danier HJ, Werner RA, Schmidt HL (1993) Correlations between the ^{13}C
520 content of primary and secondary plant products in different cell compartments
521 and that in decomposing basidiomycetes. Plant Physiol 102:1287–1290

522 Gomes SIF, Giesemann P, Klink S, et al (2023) Stable isotope natural abundances of
523 fungal hyphae extracted from the roots of arbuscular mycorrhizal
524 mycoheterotrophs and rhizoctonia-associated orchids. New Phytologist
525 239:1166–1172. https://doi.org/10.1111/nph.18990

526 Hynson NA, Madsen TP, Selosse MA, et al (2013) The physiological ecology of
527 mycoheterotrophy. In: Merckx VSFT (ed) Mycoheterotrophy: The biology of
528 plants living on fungi. Springer, Berlin, Germany, pp 297–342

529 Hynson NA, Schiebold JMI, Gebauer G (2016) Plant family identity distinguishes
530 patterns of carbon and nitrogen stable isotope abundance and nitrogen

concentration in mycoheterotrophic plants associated with ectomycorrhizal fungi. Annals of Botany 118:467–479. https://doi.org/10.1093/aob/mcw119

Jacquemyn H, Merckx VSFT (2019) Mycorrhizal symbioses and the evolution of trophic modes in plants. J Ecol 107:1567–1581. https://doi.org/10.1111/1365-2745.13165

Johansson VA, Mikusinska A, Ekblad A, Eriksson O (2015) Partial mycoheterotrophy in Pyroleae: nitrogen and carbon stable isotope signatures during development from seedling to adult. Oecologia 177:203–211. https://doi.org/10.1007/s00442-014-3137-x

Julou T, Burghardt B, Gebauer G, et al (2005) Mixotrophy in orchids: insights from a comparative study of green individuals and nonphotosynthetic individuals of *Cephalanthera damasonium*. New Phytologist 166:639–653. https://doi.org/10.1111/j.1469-8137.2005.01364.x

Kim Y-K, Jo S, Cheon S-H, et al (2020) Plastome evolution and phylogeny of Orchidaceae, with 24 new sequences. Front Plant Sci 11:22. https://doi.org/10.3389/fpls.2020.00022

Kobayashi K, Suetsugu K, Wada H (2021) The leafless orchid *Cymbidium macrorhizon* performs photosynthesis in the pericarp during the fruiting season. Plant and Cell Physiology 62:472–481. https://doi.org/10.1093/pcp/pcab006

Kumar S, Stecher G, Li M, et al (2018) MEGA X: Molecular evolutionary genetics analysis across computing platforms. Mol Biol Evol 35:1547–1549. https://doi.org/10.1093/molbev/msy096

Leake JR (1994) The biology of myco-heterotrophic ('saprophytic') plants. New Phytol 127:171–216

Maxwell K, Johnson GN (2000) Chlorophyll fluorescence - A practical guide. JExpBot 51:659–668

Mayor JR, Schuur EA, Henkel TW (2009) Elucidating the nutritional dynamics of fungi using stable isotopes. Ecology Letters 12:171–183

McCutchan Jr JH, Lewis Jr WM, Kendall C, McGrath CC (2003) Variation in trophic

560 shift for stable isotope ratios of carbon, nitrogen, and sulfur. Oikos 102:378–390.
561 https://doi.org/10.1034/j.1600-0706.2003.12098.x

562 Merckx V, Freudenstein JV (2010) Evolution of mycoheterotrophy in plants: a
563 phylogenetic perspective. New Phytologist 185:605–609.
564 https://doi.org/10.1111/j.1469-8137.2009.03155.x

565 Merckx VS, Freudenstein JV, Kissling J, et al (2013) Taxonomy and classification. In:
566 Merckx VSFT (ed) Mycoheterotrophy. Springer, Berlin, Germany, pp 19–101

567 Minagawa M, Wada E (1984) Stepwise enrichment of ^{15}N along food chains: Further
568 evidence and the relation between $\delta^{15}N$ and animal age.
569 GeochimCosmochimActa 48:1135–1140.
570 https://doi.org/10.1016/0016-7037(84)90204-7

571 Motomura H, Selosse M-A, Martos F, et al (2010) Mycoheterotrophy evolved from
572 mixotrophic ancestors: evidence in *Cymbidium* (Orchidaceae). Annals of Botany
573 106:573–581. https://doi.org/10.1093/aob/mcq156

574 Nilsson RH, Larsson K-H, Taylor AFS, et al (2019) The UNITE database for molecular
575 identification of fungi: handling dark taxa and parallel taxonomic classifications.
576 Nucleic Acids Research 47:D259–D264

577 Ogura-Tsujita Y, Yokoyama J, Miyoshi K, Yukawa T (2012) Shifts in mycorrhizal fungi
578 during the evolution of autotrophy to mycoheterotrophy in *Cymbidium*
579 (Orchidaceae). American Journal of Botany 99:1158–1176.
580 https://doi.org/10.3732/ajb.1100464

581 Ogura-Tsujita Y, Yukawa T (2008) High mycorrhizal specificity in a widespread
582 mycoheterotrophic plant, *Eulophia zollingeri* (Orchidaceae). AmJBot 95:93–97

583 Ogura-Tsujita Y, Yukawa T, Kinoshita A (2021) Evolutionary histories and mycorrhizal
584 associations of mycoheterotrophic plants dependent on saprotrophic fungi. J
585 Plant Res 134:19–41. https://doi.org/10.1007/s10265-020-01244-6

586 Op De Beeck M, Lievens B, Busschaert P, et al (2014) Comparison and validation of
587 some ITS primer pairs useful for fungal metabarcoding studies. PloS one
588 9:e97629

589 Porra RJ, Thompson WA, Kriedemann PE (1989) Determination of accurate extinction
590 coefficients and simultaneous equations for assaying chlorophylls a and b
591 extracted with four different solvents: verification of the concentration of
592 chlorophyll standards by atomic absorption spectroscopy. BBA - Bioenergetics
593 975:384–394

594 Rasmussen HN, Rasmussen FN (2014) Seedling mycorrhiza: a discussion of origin and
595 evolution in Orchidaceae. BotJLinnSoc 175:313–327

596 Ritchie GA (2006) Chlorophyll fluorescence: What is it and what do the numbers mean?
597 USDA Forest Service Proceedings RMRS 43:34–43

598 Roy M, Gonneau C, Rocheteau A, et al (2013) Why do mixotrophic plants stay green? A
599 comparison between green and achlorophyllous orchid individuals in situ. Ecol
600 Monogr 83:95–117

601 Sakamoto Y, Ogura-Tsujita Y, Ito K, et al (2016) The tiny-leaved orchid *Cephalanthera*
602 *subaphylla* obtains most of its carbon via mycoheterotrophy. Journal of Plant
603 Research 129:1013–1020

604 Schiebold JMI, Bidartondo MI, Karasch P, et al (2017) You are what you get from your
605 fungi: Nitrogen stable isotope patterns in *Epipactis* species. AnnBot
606 119:1085–1095. https://doi.org/10.1093/aob/mcw265

607 Schweiger JMI, Bidartondo MI, Gebauer G (2018) Stable isotope signatures of
608 underground seedlings reveal the organic matter gained by adult orchids from
609 mycorrhizal fungi. Funct Ecol 32:870–881

610 Selosse MA, Faccio A, Scappaticci G, Bonfante P (2004) Chlorophyllous and
611 achlorophyllous specimens of *Epipactis microphylla* (Neottieae, Orchidaceae)
612 are associated with ectomycorrhizal septomycetes, including truffles. Microb
613 Ecol 47:416–426

614 Selosse M-A, Roy M (2009) Green plants that feed on fungi: facts and questions about
615 mixotrophy. Trends Plant Sci 14:64–70.
616 https://doi.org/10.1016/j.tplants.2008.11.004

617 Stöckel M, Meyer C, Gebauer G (2011) The degree of mycoheterotrophic carbon gain
618 in green, variegated and vegetative albino individuals of *Cephalanthera*

619 *damasonium* is related to leaf chlorophyll concentrations. New Phytologist
620 189:790–796. https://doi.org/10.1111/j.1469-8137.2010.03510.x

621 Suetsugu K, Haraguchi TF, Okada H, Tayasu I (2021a) *Stigmatodactylus sikokianus*
622 (Orchidaceae) mainly acquires carbon from decaying litter through association
623 with a specific clade of Serendipitaceae. New Phytologist 231:1670–1675.
624 https://doi.org/10.1111/nph.17523

625 Suetsugu K, Haraguchi TF, Tanabe AS, Tayasu I (2021b) Specialized mycorrhizal
626 association between a partially mycoheterotrophic orchid *Oreorchis indica* and a
627 *Tomentella* taxon. Mycorrhiza 31:243–250

628 Suetsugu K, Haraguchi TF, Tayasu I (2022) Novel mycorrhizal cheating in a green
629 orchid: *Cremastra appendiculata* depends on carbon from deadwood through
630 fungal associations. New Phytol 235:333–343.
631 https://doi.org/10.1111/nph.17313

632 Suetsugu K, Matsubayashi J (2021a) Evidence for mycorrhizal cheating in *Apostasia*
633 *nipponica*, an early-diverging member of the Orchidaceae. New Phytol
634 229:2302–2310

635 Suetsugu K, Matsubayashi J (2021b) Subterranean morphology modulates the degree of
636 mycoheterotrophy in a green orchid *Calypso bulbosa* exploiting wood-decaying
637 fungi. Functional Ecology 35:2305–2315.
638 https://doi.org/10.1111/1365-2435.13864

639 Suetsugu K, Matsubayashi J (2022) Foliar chlorophyll concentration modulates the
640 degree of fungal exploitation in a rhizoctonia-associated orchid. Journal of
641 Experimental Botany 73:4204–4213

642 Suetsugu K, Matsubayashi J, Tayasu I (2020) Some mycoheterotrophic orchids depend
643 on carbon from dead wood: Novel evidence from a radiocarbon approach. New
644 Phytol 227:1519–1529. https://doi.org/10.1111/nph.16409

645 Suetsugu K, Ohta T, Tayasu I (2018) Partial mycoheterotrophy in the leafless orchid
646 *Cymbidium macrorhizon*. Am J Bot 105:1595–1600

647 Suetsugu K, Yamato M, Matsubayashi J, Tayasu I (2021c) Partial and full
648 mycoheterotrophy in green and albino phenotypes of the slipper orchid

649 *Cypripedium debile*. Mycorrhiza 31:301–312.
650 https://doi.org/10.1007/s00572-021-01032-7

651 Suetsugu K, Yamato M, Miura C, et al (2017) Comparison of green and albino
652 individuals of the partially mycoheterotrophic orchid *Epipactis helleborine* on
653 molecular identities of mycorrhizal fungi, nutritional modes and gene expression
654 in mycorrhizal roots. Mol Ecol 26:1652–1669.
655 https://doi.org/10.1111/mec.14021

656 Syed F, Grunenwald H, Caruccio N (2009) Optimized library preparation method for
657 next-generation sequencing. NatMethod 6:1–2

658 Tanabe AS, Toju H (2013) Two new computational methods for universal DNA
659 barcoding: A benchmark using barcode sequences of bacteria, archaea, animals,
660 fungi, and land plants. PLoS ONE 8:e76910.
661 https://doi.org/10.1371/journal.pone.0076910

662 Tayasu I, Hirasawa R, Ogawa NO, et al (2011) New organic reference materials for
663 carbon- and nitrogen-stable isotope ratio measurements provided by Center for
664 Ecological Research, Kyoto University, and Institute of Biogeosciences, Japan
665 Agency for Marine-Earth Science and Technology. Limnology 12:261–266.
666 https://doi.org/10.1007/s10201-011-0345-5

667 Taylor DL, McCormick MK (2008) Internal transcribed spacer primers and sequences
668 for improved characterization of basidiomycetous orchid mycorrhizas. New
669 Phytologist 177:1020–1033. https://doi.org/10.1111/j.1469-8137.2007.02320.x

670 Trudell SA, Rygiewicz PT, Edmonds RL (2003) Nitrogen and carbon stable isotope
671 abundances support the myco-heterotrophic nature and host-specificity of certain
672 achlorophyllous plants. New Phytologist 160:391–401.
673 https://doi.org/10.1046/j.1469-8137.2003.00876.x

674 Tsukaya H (2018) How have leaves of mycoheterotrophic plants evolved–from the view
675 point of a developmental biologist. New Phytol 217:1401–1406

676 Waud M, Busschaert P, Ruyters S, et al (2014) Impact of primer choice on
677 characterization of orchid mycorrhizal communities using 454 pyrosequencing.
678 Mol Ecol Resour 14:679–699. https://doi.org/10.1111/1755-0998.12229

679 Yagame T, Lallemand F, Selosse M-A, et al (2021) Mycobiont diversity and first
680 evidence of mixotrophy associated with Psathyrellaceae fungi in the
681 chlorophyllous orchid *Cremastra variabilis*. Journal of Plant Research
682 134:1213–1224

683 Zahn FE, Lee Y-I, Gebauer G (2022) Fungal association and root morphology shift
684 stepwise during ontogenesis of orchid *Cremastra appendiculata* towards
685 autotrophic nutrition. AoB Plants 14:plac021

686 Zahn FE, Söll E, Chapin TK, et al (2023) Novel insights into orchid mycorrhiza
687 functioning from stable isotope signatures of fungal pelotons. New Phytologist
688 239:1449–1463. https://doi.org/10.1111/nph.18991

689 Zanden MJ, Rasmussen JB (2001) Variation in $\delta^{15}N$ and $\delta^{13}C$ trophic fractionation:
690 Implications for aquatic food web studies. LimnolOceanogr 46:2061–2066.
691 https://doi.org/10.4319/lo.2001.46.8.2061

692 Zimmer K, Meyer C, Gebauer G (2008) The ectomycorrhizal specialist orchid
693 *Corallorhiza trifida* is a partial myco-heterotroph. New Phytologist
694 178:395–400. https://doi.org/10.1111/j.1469-8137.2007.02362.x

695

696

Figure legends

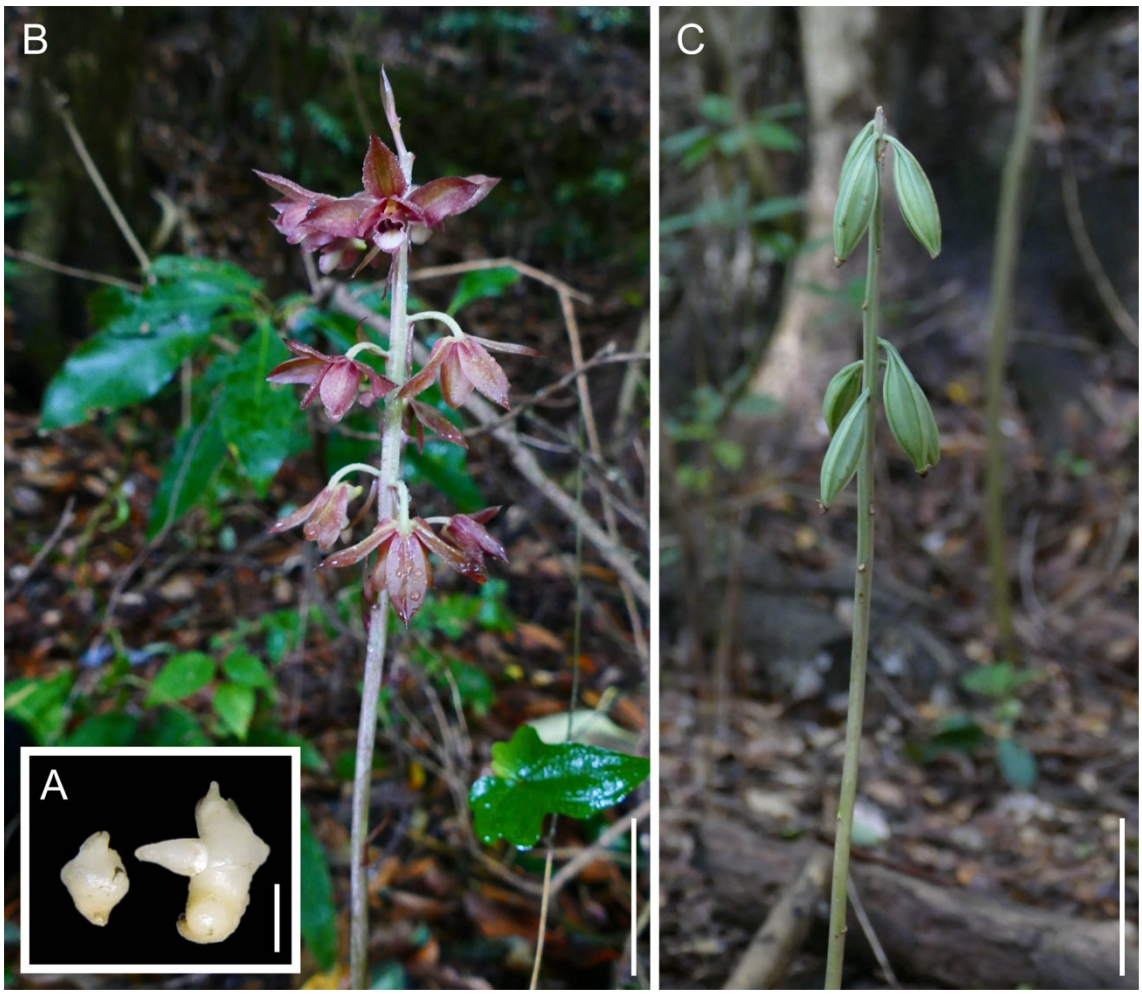

Figure 1. Life history of *Eulophia zollingeri.* (A) Protocorms. (B) Flowering plant. (C) Fruiting plant. Scale bars: 5 mm (A) and 30 mm (B–C).

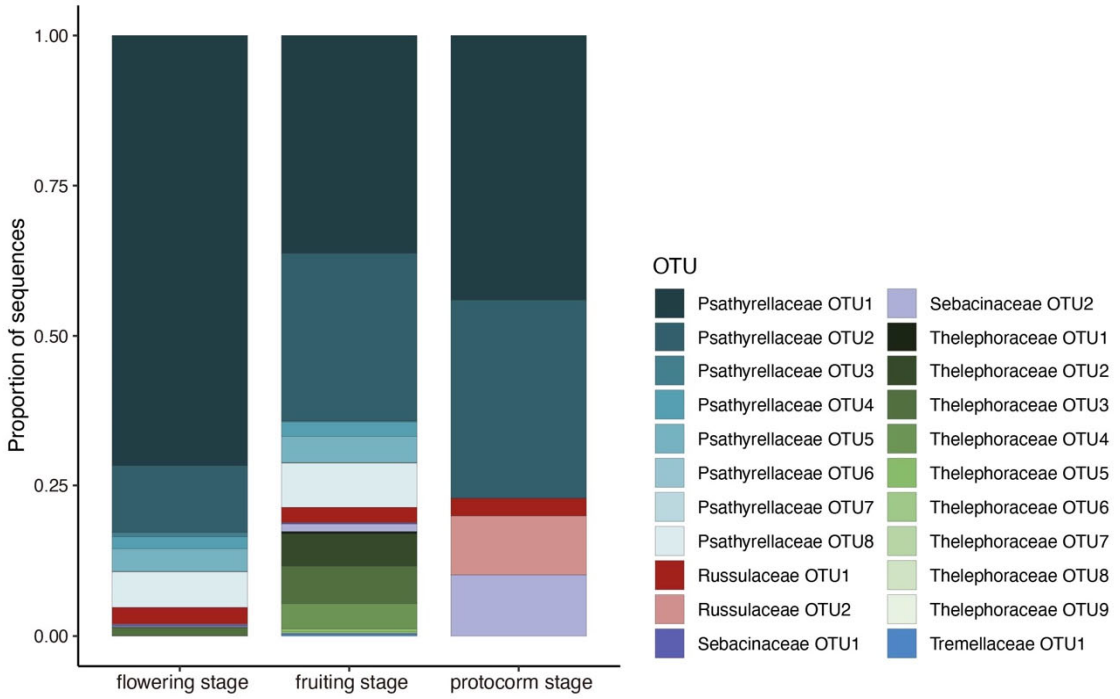

Figure 2. Relative abundance of mycorrhizal fungi DNA sequence reads amplified from *Eulophia zollingeri* across three stages (protocorm, flowering, and fruiting stages) at the operational taxonomic unit (OTU) level.

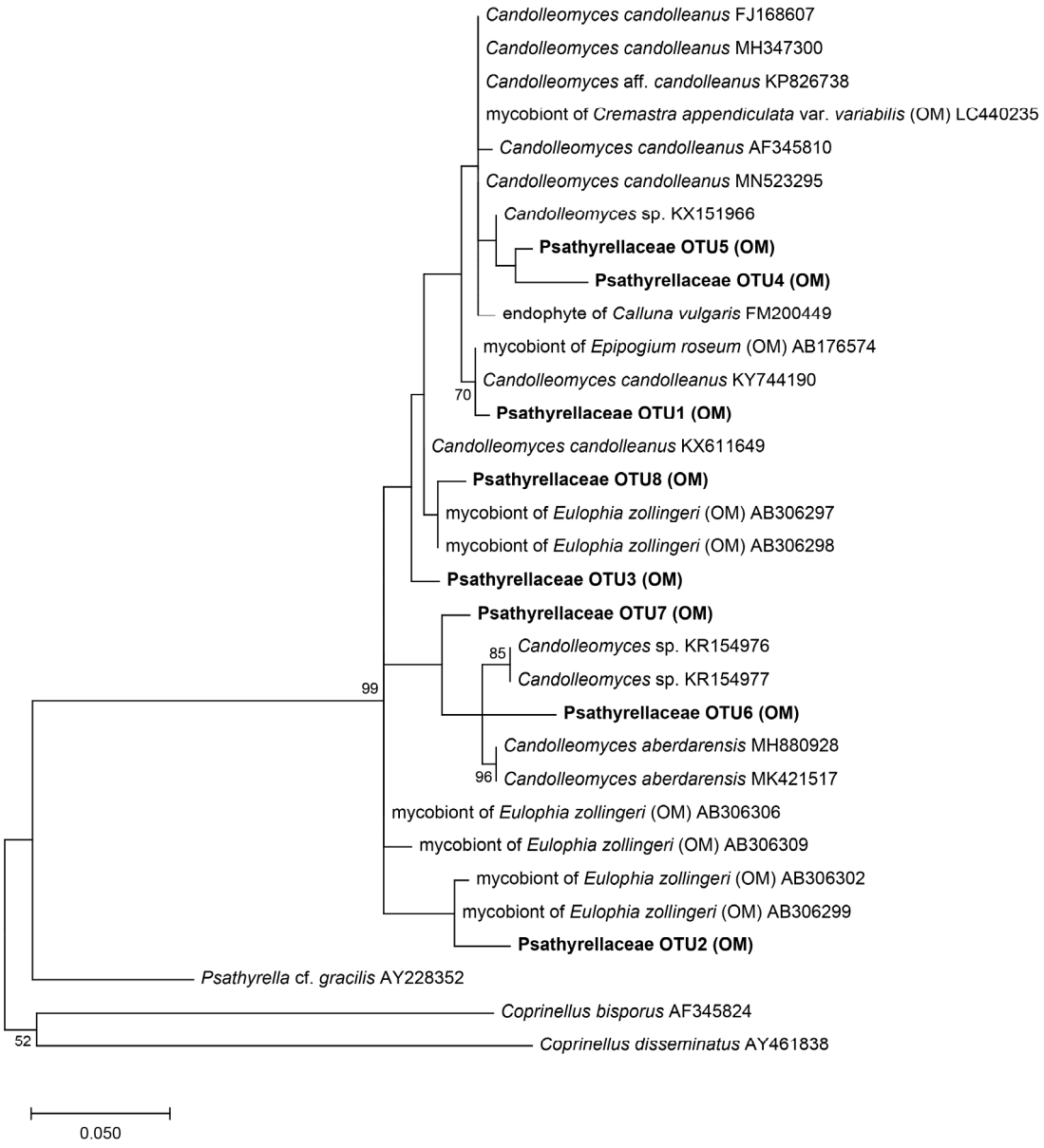

706

707 **Figure 3.** Maximum-likelihood phylogenetic tree of ITS2 rDNA sequences from
708 Psathyrellaceae fungi detected in mycorrhizal samples of *Eulophia zollingeri* in the
709 present study (bold typeface), along with sequences obtained from the INSDC database.
710 Accession numbers are provided for all INSDC sequences. The maximum-likelihood
711 tree was rooted using *Coprinellus bisporus* and *C. disseminatus* (Psathyrellaceae). Node
712 values indicate bootstrap values (1000 replicates) of 50% or greater. The scale bar
713 indicates the number of substitutions per site.

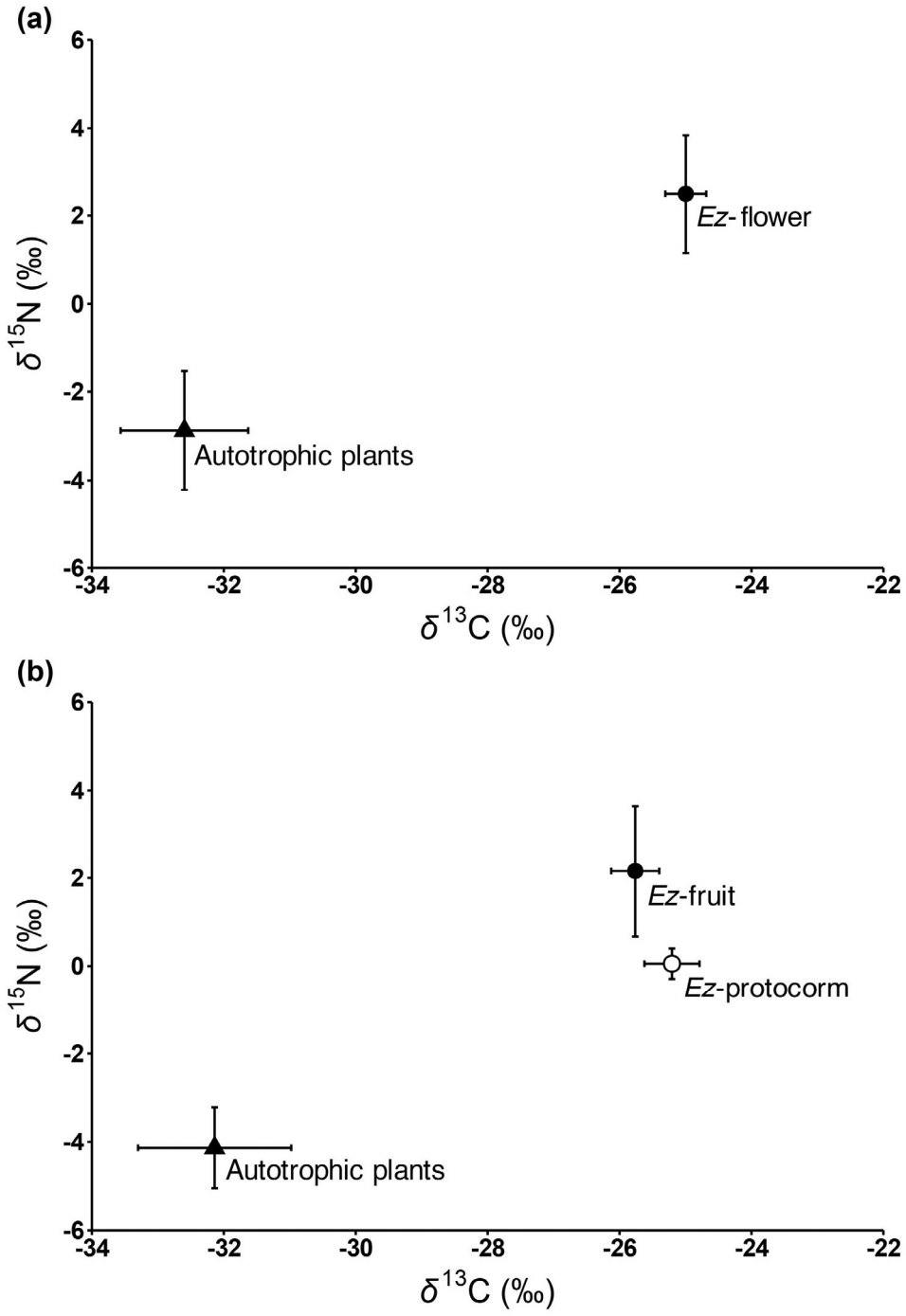

714

715 **Figure 4.** Mean (± SD) $\delta^{13}C$ and $\delta^{15}N$ values of *Eulophia zollingeri* and its neighboring
716 autotrophic plants during the (a) flowering season and (b) fruiting season.
717 *Ez*-protocorm: *E. zollingeri* specimens at the protocorm stage. *Ez*-flower: *E. zollingeri*
718 specimens at the flowering stage. *Ez*-fruit: *E. zollingeri* specimens at the fruiting stage.